Structural studies of side-chain liquid crystal polymers and elastomers

G. R. Mitchell, F. J. Davis and A. Ashman
J. J. Thomson Physical Laboratory and Department of Chemistry, University of Reading, Whiteknights, Reading RG6 2AF, UK
(Received 15 September 1986; revised 9 January 1987; accepted 10 January 1987)

The preparation of a range of acrylate-based side-chain liquid crystal elastomers is described. Materials containing up to 13 mol% of crosslinking units exhibit a nematic–isotropic transition. In the isotropic phase the mechanical properties are similar to those observed in conventional elastomers, and are used to obtain an estimate of the level of effective crosslinking. Wide-angle X-ray scattering procedures are employed to obtain structural information on macroscopically unaligned and aligned samples, the alignment being introduced by mechanical means. Analysis of the scattering from aligned samples shows that although the coupling chain length is short, the mesogenic side-chains are preferentially aligned in the direction of extension. Furthermore, the analysis shows that a considerable number of the coupling chains adopt *gauche* isomers. A more detailed examination of the alignment process shows that only a few percent extension is necessary to achieve high levels of molecular alignment, when the deformation is performed in the liquid crystal phase. Attention is drawn to the parallel with electro-optic and magneto-optic effects.

(Keywords: liquid crystal polymer; liquid crystal elastomer; X-ray scattering; molecular switching; molecular organization)

INTRODUCTION

There is now a wide range of synthetic side-chain polymers that exhibit thermotropic liquid crystal phases[1,2]. The basic building blocks of this type of material are well established, namely the flexible polymer backbone, the rigid 'mesogenic' unit and a short chain to join those two components. Initially it was suggested that the short connecting chain decoupled the mesogenic unit from the polymer backbone and that was a prerequisite to the formation of a liquid crystal phase. It is now clear that there are varying levels of coupling between the components of a side-chain liquid crystal polymer, which are dependent upon its chemical configuration. For example, neutron-scattering studies[3] show that the polymer backbone undergoes some reorientation in a magnetic field in addition to the mesogenic units. The temperature dependence of the electric-field response times may be related to the temperature sensitivity of the viscosity of the bulk polymer[4,5]. Furthermore the electro-optic response of side-chain liquid crystal polymers is particularly sensitive to the thermal/chronal history of each sample, and this may be related to the coupling of the side-chain organization to the very long relaxation times of the polymer backbone[5]. We may further affect the influence of the polymer backbone chains upon the properties of a liquid crystal polymer by linking those chains together to form a polymer network, and hence a liquid crystal elastomer[6,7]. This contribution is concerned with the molecular organization of such liquid crystal elastomers and their properties. In particular, we shall report studies made on liquid crystal elastomers based upon an acrylate backbone and in which the coupling chain is short to maximize the interaction between mesogenic unit and polymer backbone chain. These materials behave as conventional elastomers when in the isotropic phase, but show markedly different mechanical properties when deformed in the liquid crystal phase. X-ray scattering techniques are used to monitor the level of anitotropy induced and to obtain structural detail.

MATERIALS

The essential components of a side-chain liquid crystal elastomer are shown schematically in *Figure 1*. Thus, in addition to the mesogenic unit, the coupling chain and the polymer backbone of a 'normal' side-chain liquid crystal polymer, we must add crosslinking units to join different polymer backbone chains together. We may choose to add crosslinking chains to the free ends of the mesogenic side-chains (*Figure 2a*) or we may use a non-mesogenic crosslinking sub-chain to join the polymer backbones (*Figure 2b*). In this study we have selected the latter method. In addition, there is a choice of crosslinking a polymeric material, as, for example, in the vulcanization of conventional rubbers, or to allow the crosslinking to proceed during polymerization, which is the method used in this study. This is achieved by copolymerization, in which one of the monomers (*Figure 3a*) contains the mesogenic unit and the other is a difunctional moiety (*Figure 3b*). In this study both the coupling chain between the polymer backbone and the mesogenic unit (n) and the crosslinking chain (m) contained two methylene groups. The level of crosslinking may be varied by adjusting the ratio of the comonomers. The detailed preparation and characterization of these materials is described elsewhere[7,8].

The first need is to establish the copolymer compositions that exhibit enantiotropic liquid crystal phases. A range of materials was synthesized containing from 0 to 40% of the crosslinking chain. Only those containing less than 15% of the crosslinking chain displayed a nematic–isotropic transition, although

0032-3861/87/040639-09$03.00

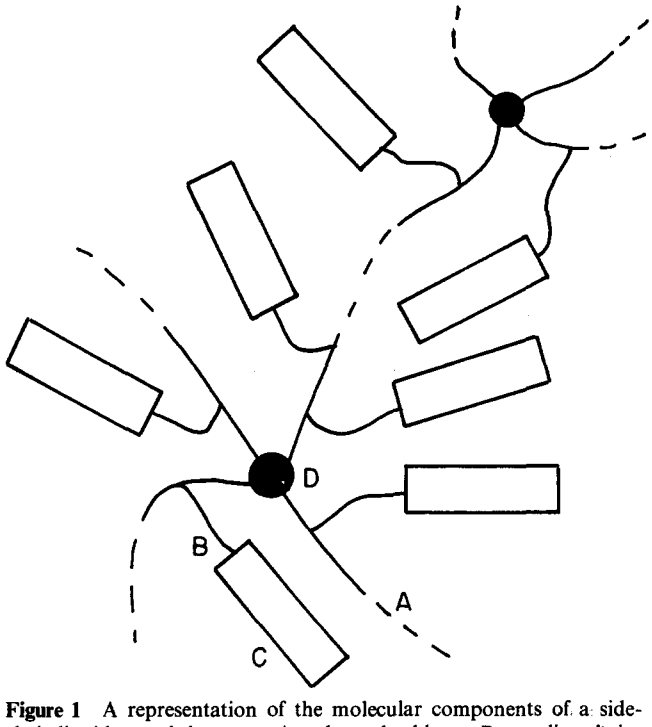

Figure 1 A representation of the molecular components of a side-chain liquid crystal elastomer: A, polymer backbone; B, coupling chain; C, mesogenic unit; D, chemical crosslink

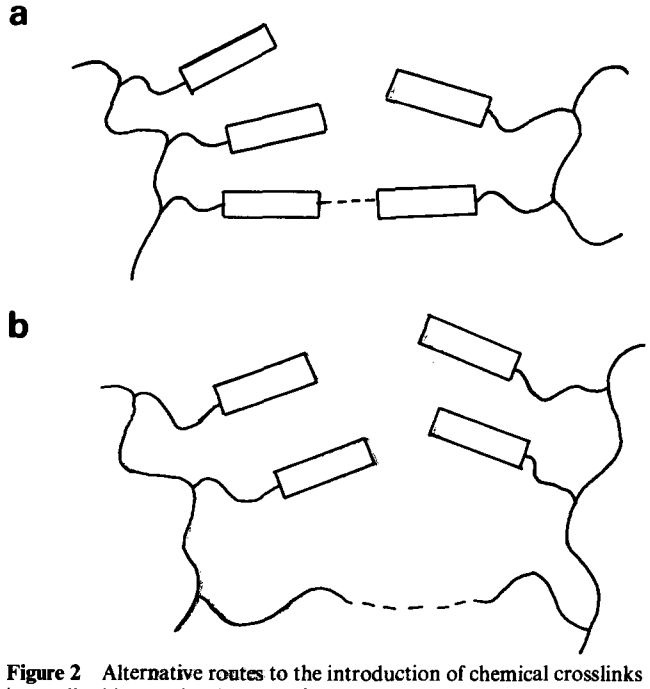

Figure 2 Alternative routes to the introduction of chemical crosslinks into a liquid crystal polymer to form an elastomer

copolymers with higher than 15 mol% concentration of the linking chain displayed birefringent textures. The latter materials are similar in essence to those described some years ago by Liebert and co-workers[9]. The effect of copolymerization was to increase the glass-transition and lower the nematic–isotropic transition, as indicated in *Table 1*. The copolymer composition does not directly correspond to the level of crosslinking; that would only be correct if the copolymerization was random and if no intramolecular looping is introduced. The first consideration would appear very reasonable for radical polymerization, and we know from kinetic studies[8] that the reactivities of our two monomers are very similar. However, it is known that crosslinking in dilute solution promotes intramolecular linkages. That these occur may be deduced from an inspection of *Table 1*. We would normally expect materials with those nominal crosslink densities to be intractable, yet those prepared display a mobile liquid crystal phase. In the isotropic phase the liquid crystal elastomers appear to behave as conventional elastomers, i.e. they exhibit large-scale reversible elastic deformation. For a conventional elastomer with a perfectly formed network, we may relate its modulus to the molecular weight between crosslink points by[10]

$$G = RT\rho/M_s \qquad (1)$$

where M_s is the number-average of the chain section between two junction points, ρ is the bulk density, T the temperature and R the gas constant. *Figure 4* shows the moduli measured at *ca.* 150°C (i.e. above the nematic–isotropic transition temperature for the series of elastomers, including both those which exhibited a nematic–isotropic phase transition and those which did not. Also drawn is the expected modulus *versus* crosslink density relation calculated from equation (1) and by assuming a perfectly formed network. It is clear that all the materials show a lower modulus than would directly relate to the comonomer composition. From this plot the crosslink density is between a third and a sixth of that indicated by the copolymer composition. However, the interpretation of the modulus values is complicated by the possibility of pretransitional effects for those elastomers which exhibit a liquid crystal phase[6,8], indeed such effects may explain the apparent step in the modulus at a nominal 13 mol% fraction of crosslinking unit. In the remainder of this paper we shall consider the molecular organization and mechanical properties, principally of an elastomer with a nominal crosslinking density of 3.5%, which relates to an effective crosslink density of *ca.* 1%

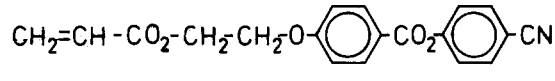

a

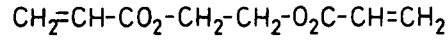

b

Figure 3 The mesogenic monomer (a) and the crosslinking monomer (b) used in this study

Table 1 Thermal characteristics[a] of copolymers used in this study[8]

Molar fraction of crosslinking chain	Glass transition (°C)	Nematic–isotropic (°C)
0	74.4	110.1
2.8	75.2	103.4
6.9	77.8	100.4
10.0	80.2	105.8
13.6	82.1	97.2
26.3	86.9	nto
37.8	102.1	nto
48.6	nto	nto

[a] Transition temperatures measured with a Perkin-Elmer DSC2 with heating rate of 10 K min^{-1}

[b] nto: no transition observed before thermal decomposition

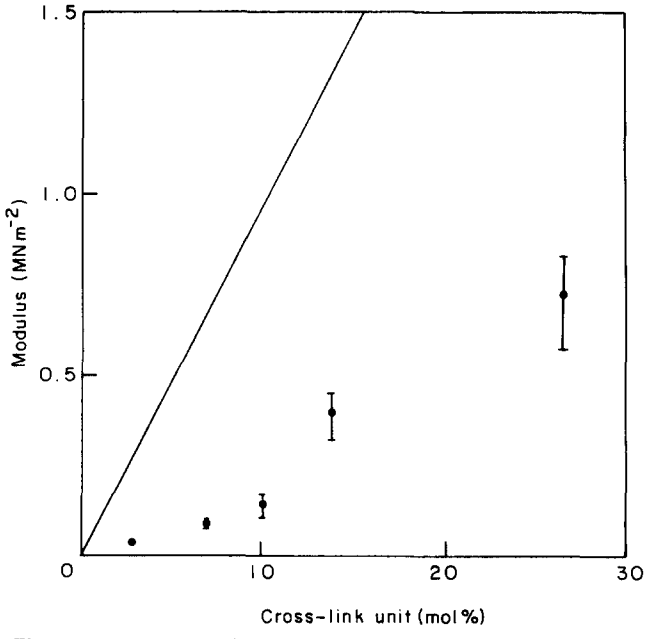

Figure 4 The measured values of the initial modulus of liquid crystal elastomers deformed in the isotropic phase (*ca.* 150°C) plotted as a function of the copolymer composition. The solid line corresponds to the predicted modulus obtained by using equation (1) and assuming a perfectly formed network

EXPERIMENTAL

X-ray scattering and mechanical measurements were made on free-standing films of thickness *ca.* 0.5 mm. These films were prepared by moulding under pressure, followed by a thermal treatment at 150°C to bring the material to a starting relaxed state. For the mechanical measurements the thin films were sliced into strips while at a temperature within the isotropic phase. The preparation of aligned samples and the mechanical testing was achieved by using a 'Microscope Tensile Tester' from Rosand Precision Ltd fitted with a 20 N force transducer and interfaced to a microcomputer. The samples were heated in the mechanical testing device by using hot air within a small oven, the temperature being controlled to ± 1°C.

The structural studies employed wide-angle X-ray scattering techniques and were made on a computer-controlled 3-circle transmission diffractometer[11]. The diffractometer (*Figure 5*) was operated in a symmetrical transmission geometry, and was equipped with an incident-beam monochromator and pinhole collimation and a third circle which allowed the sample to be rotated in its own plane, i.e. a plane normal to the plane containing the incident and scattered paths. This circle was used in the study of samples with a preferred global orientation. Measurements of the scattered intensity from the liquid-crystal elastomers were made at room temperature, i.e. on glassy samples. Those samples had been rapidly cooled by an air jet from their preparation temperature, and optical microscopy showed that the microstructure consistent with the elevated temperatures was retained in the glass. The X-ray scattered intensity was measured over the range $s \approx 0.3$ to 6.3 $Å^{-1}$, where $s = 4\pi \sin\theta/\lambda$ and 2θ is the angle between the incident and scattered beams. For samples with a preferred global orientation, the scattered intensity was also measured as a function of α, the angle between the symmetry axis of the sample (the extension axis) and the normal to the plane containing incident and scattered beams. Those measurements were made from $\alpha = 0°$ to 90° in steps of 9°.

X-RAY SCATTERING ANALYSIS

Unaligned samples

Figure 6 shows the measured scattered intensity functions for the homopolymer (uncrosslinked) and for two crosslinked samples. These samples were quenched from the liquid crystal phase, they exhibit no global molecular orientation, but of course contain local alignment commensurate with a nematic structure, as may be observed by using polarizing microscopy. All three curves shown in *Figure 6* are essentially the same:

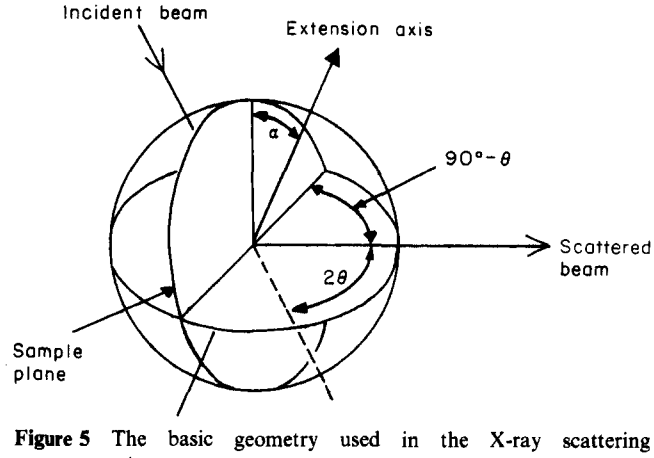

Figure 5 The basic geometry used in the X-ray scattering measurements

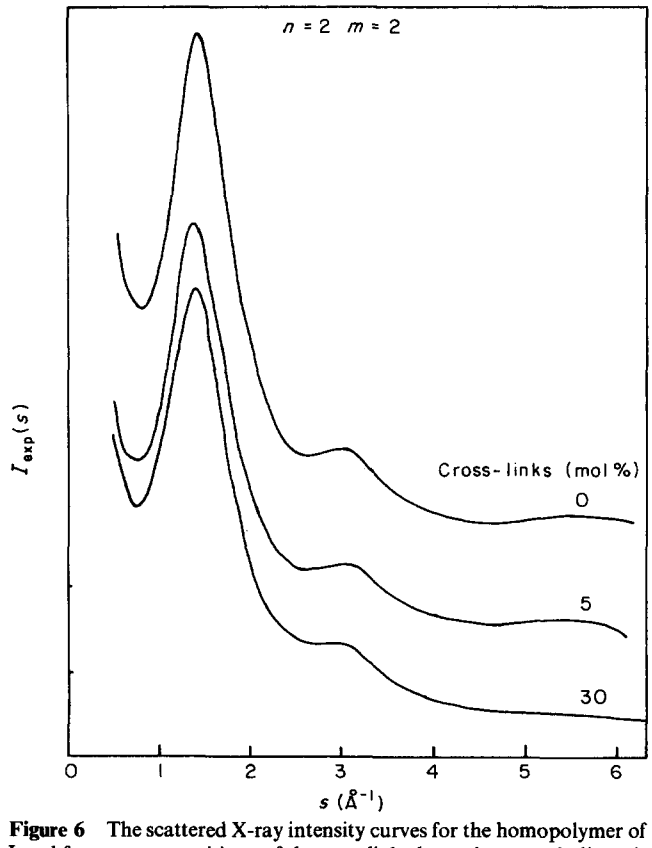

Figure 6 The scattered X-ray intensity curves for the homopolymer of I and for two compositions of the crosslinked copolymer as indicated. The measurements were made at room temperature on samples cooled from the nematic phase where appropriate. The samples had no macroscopic molecular orientation. $s = 4\pi \sin\theta/\lambda$ where 2θ is the angle between the scattered and incident paths

each contains an intense peak at $s \approx 1.5$ Å^{-1}, which we would relate to the spatial correlations between mesogenic units, and weaker peaks at $s \approx 3$ and 5.5 Å^{-1}. These higher scattering-vector peaks are related to correlations within the constituent parts of the liquid crystal polymer. As the level of crosslinking increases these higher scattering-vector peaks become weaker; this is simply related to the difference between the intrachain scattering of the mesogenic repeat and the crosslinking unit. We may qualitatively characterize the intense interchain peak at $s \approx 1.5$ Å^{-1} by the position of its maximum intensity and the breadth of the peak at half that intensity. These two parameters are plotted as a function of the concentration of the crosslink unit in *Figure 7*. These plots reinforce the view from *Figure 6* that the introduction of crosslinking units does not significantly alter the near-neighbour structure from that of the homopolymer.

Aligned samples

The utility of wide-angle X-ray scattering analysis is considerably enhanced by the use of samples with a high level of preferred molecular orientation. Such X-ray procedures will provide quantitative measures of the level of molecular orientation, in addition to an evaluation of the molecular organization. We have prepared samples with a global molecular anisotropy through the use of mechanically induced molecular switching[12] and this is described in a later section. *Figure 8* shows the s-weighted reduced intensity function $si(s,\alpha)$ obtained for a sample macroscopically aligned by an extension ratio of 2. This scattering function is the experimental data, which have

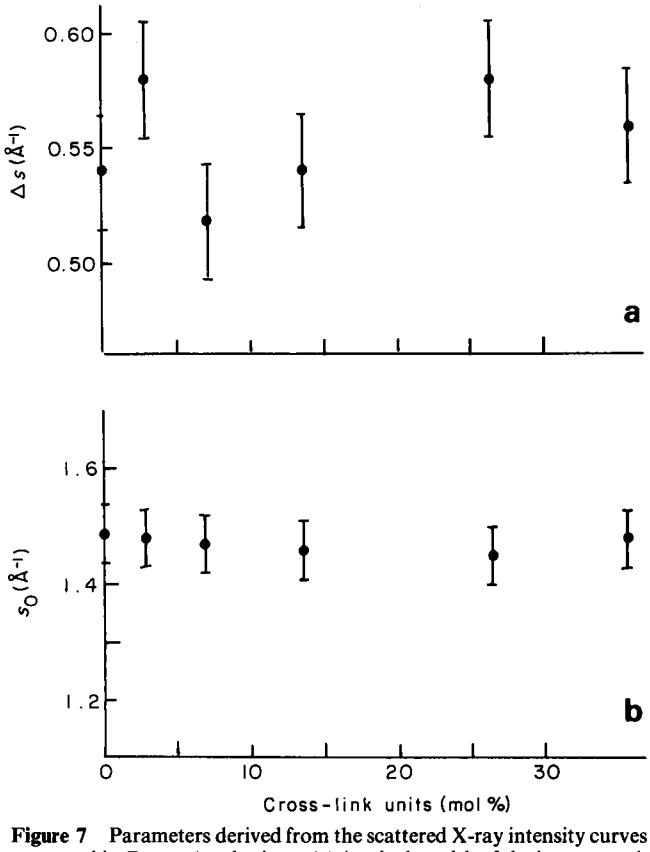

Figure 7 Parameters derived from the scattered X-ray intensity curves presented in *Figure 6* and others: (a) Δs, the breadth of the intense peak at $s \approx \approx 1.5$ Å^{-1}, measured at half the peak intensity value and (b) s_0, the position of the intense peak, plotted as a function of the copolymer composition

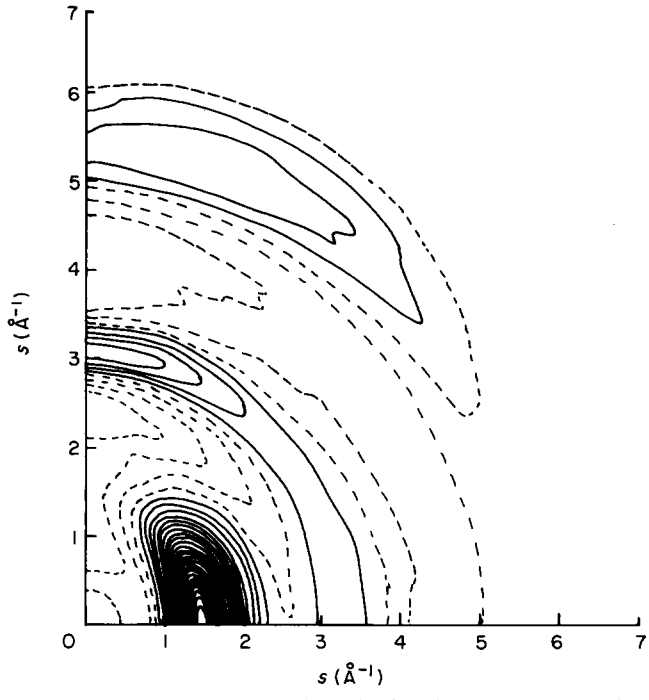

Figure 8 The scattered X-ray intensity function $si(s,\alpha)$ measured at room temperature for a copolymer containing a nominal 2.8% of the crosslinking unit, corresponding to an effective crosslinking density of *ca.* 1%. The sample was rapidly cooled from 85°C, following a mechanical extension of 100%. The extension axis is vertical. The broken contours represent negative values of the intensity function. The function was prepared by using the procedures detailed in references 11 and 13

been corrected for experimental aberrations, normalized to electron units, and from which the independent scattering component has been subtracted by using the procedures detailed in references 11 and 13. The marked anisotropy of the molecular organization in this sample is clearly shown by the intensification of the peak at $s \approx 1.5$ Å^{-1} onto the equatorial section (i.e. normal to the extension axis). As this peak arises from the spatial correlations between mesogenic units, the fact that it is most intense on the section normal to the extension axis directly indicates that the mesogenic units are aligned parallel to the extension axis. The peaks at $s \approx 3$ and 5.5 Å^{-1} are most intense on the meridional section (i.e. parallel to the extension axis), and since these arise principally from correlations within a mesogenic unit, their intensification confirms that the mesogenic units are indeed aligned parallel to the extension axis. We may by appropriate analysis extract considerably more quantitative structural information from this higher scattering-vector intensity data. In the following section we present the basic procedures used, which are considered in more detail elsewhere[11,13,14].

Basic scattering theory

The scattering function $si(s,\alpha)$ shown in *Figure 8* for a partially aligned sample of a liquid crystal elastomer may be considered as the convolution of a perfectly aligned sample $si^m(s,\alpha)$ and the orientation distribution function $D(\alpha)$:

$$si(s,\alpha) = si^m(s,\alpha) * D(\alpha) \qquad (2)$$

We consider here only samples with uniaxial symmetry. This convolution is only valid when we consider the scattering from isolated units, rather than interunit

scattering. Such a proviso applies to the scattering at high scattering vectors from disordered polymer samples, as has been illustrated on a number of occasions[13,15]. If we express each of the functions in equation (2) by a series of Legendre polynomials (of even order due to symmetry) then we may write the convolution as[13,16]:

$$si_{2n}(s) = si^{m}_{2n}(s) \cdot (4n + 1/2\pi) \cdot D_{2n} \quad (3)$$

where

$$si_{2n}(s) = 4n + 1 \int_0^{\pi/2} si(s, \alpha) \sin \alpha P_{2n}(\cos \alpha)\, d\alpha \quad (4)$$

and P_{2n} are Legendre polynomials*. Analagous relationships to equation (4) may be written for D_{2n} and for $si^{m}_{2n}(s)$. The advantages of this approach are clear from equation (3). The observed spherical harmonics, $si_{2n}(s)$, are those of a perfectly aligned system weighted with coefficients that depend only upon the level of orientation of the structural units. Thus in terms of peak positions, peak breadths and relative peak heights, the observed coefficients are identical with those of a perfectly aligned unit. It is only in terms of their absolute intensity that they will differ. In fact if we know $si^{m}_{2n}(s)$ we may deduce the values of D_{2n} and hence the orientation distribution function[14,16]. We shall exploit equation (3) for structural information by comparing the observed spherical harmonics $si_{2n}(s)$ with those calculated for models of perfectly aligned structural units, bearing in mind the restrictions of the scattering-vector range and of the items detailed above.

The orientation parameter, $\langle P_2 \rangle$, values were obtained by using the measured anisotropy of the intense peak at $s \approx 1.5$ Å^{-1} by using procedures detailed in references 11, 14 and 16.

Side-chain conformation

Figure 9 shows the first three spherical harmonics derived from the experimental scattering function shown in *Figure 8*, by using equation (4). We shall adopt as a starting structural unit the repeat unit of the mesogenic monomer as shown in *Figure 10*. In this example we have aligned the mesogenic unit to be normal to the symmetry axis z. *Figure 11* shows the first three spherical harmonics calculated from such a model. Note that the intense peak at $s \approx 1.5$ Å^{-1} is absent, and this is expected since that peak arises from interunit correlations and our model only contains one unit. If we compare these functions with those derived from the experimental scattering data (*Figure 9*), bearing in mind the restrictions of such a comparison, it is clear that there is little match between the two sets of functions. That is apart from the match between the components for $n = 0$. These components are the isotropic terms and hence do not depend upon the axis of alignment of the system. That there is tentative agreement suggests we have broadly the correct structural unit, but an incorrect alignment. If the structural unit is aligned such that the C–N bond is parallel to the symmetry or z-axis, as shown in *Figure 12*, then we obtain the spherical harmonics shown in *Figure 13*. A comparison of those functions with the experimental functions (*Figure 9*) is much better. The

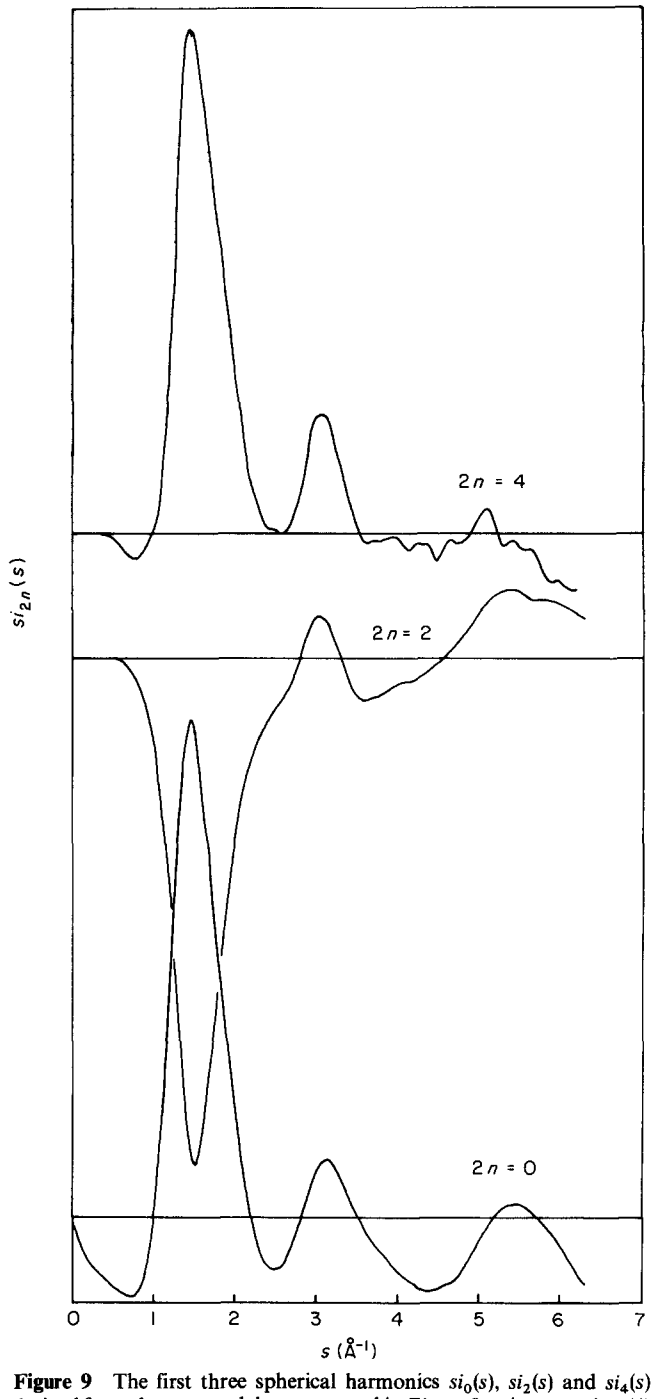

Figure 9 The first three spherical harmonics $si_0(s)$, $si_2(s)$ and $si_4(s)$ derived from the scattered data presented in *Figure 8*, using equation (4) in the text

positions of the peaks and their sign is in good accord with the experimental functions. However, many of the features in the model functions are too sharp and too intense, for example the peak at $s \approx 5.5$Å^{-1} in $si_4(s)$. This would suggest that our structural unit is too regular and some disorder is required.

We have taken as the starting unit the most extended mesogenic unit conformation. Structural disorder may be introduced by the rotation of the phenyl groups, but this will have little effect upon the X-ray scattering since such rotations do not significantly change interatomic distances. The most marked conformational disorder that may be introduced in the repeat unit is the conformational sequence of the bonds making up the coupling chain, i.e. O–CH_2–CH_2–O. In the initial

* $P_0(\cos \alpha) = 1$
$P_2(\cos \alpha) = (3 \cos^2 \alpha - 1)/2$
$P_4(\cos \alpha) = (35 \cos^4 \alpha - 30 \cos^2 \alpha + 3)/8$

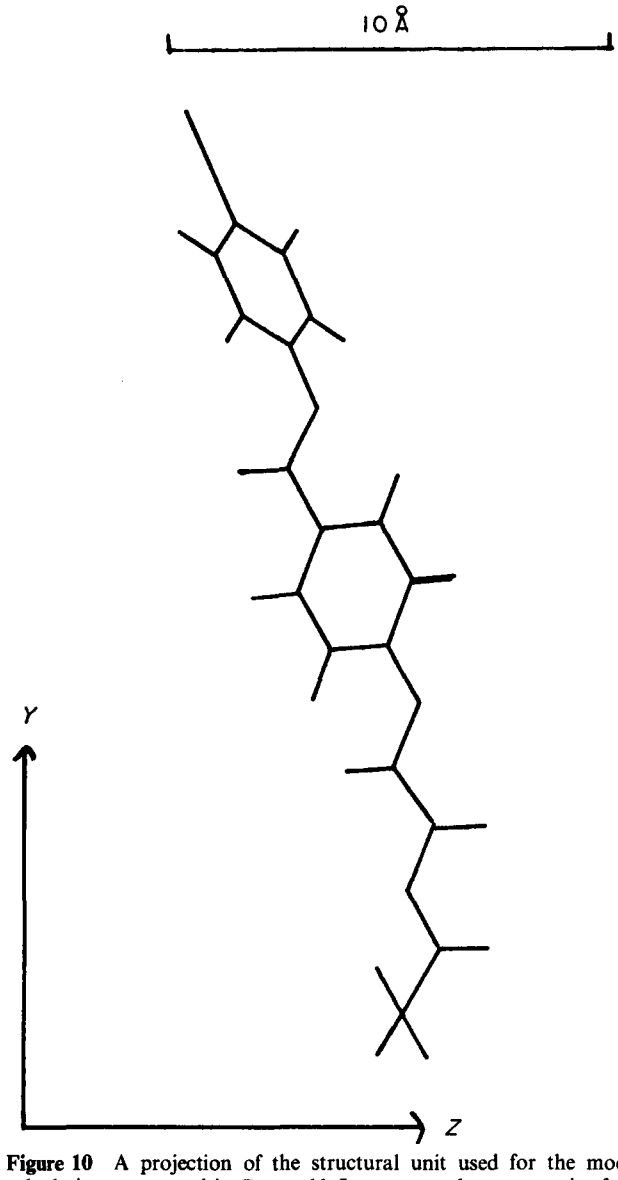

Figure 10 A projection of the structural unit used for the model calculations presented in *Figure 11*. It corresponds to one unit of the mesogenic repeat (*Figure 3a*) with the coupling chain fully extended. It is aligned normal to the extension axis z

structural unit these bonds have been placed in the extended form, as observed in crystal structures of model compounds[17,18]. *Figure 14* shows the harmonics calculated for a model, still with C–N bonds parallel to the z-axis, but in which *gauche* isomers have been introduced into the coupling chain. The comparison between model and experiment is much improved, particularly in terms of the peak at $s \approx 5.5$ Å^{-1}. This shows directly that the coupling chains are far from being extended, and hence the mesogenic units are not simply at right-angles to the polymer backbone. A more detailed model with a statistical distribution of the various side-chain conformations is being developed and will be reported later.

The molecular alignment was introduced by stretching the liquid crystal elastomer, and this would introduce some alignment of the polymer backbone chains. Since there is close coupling between the mesogenic unit and the polymer backbone, we might have expected that such polymer backbone alignment would lead to a preferred orientation of the mesogenic units normal to the chain alignment and hence the extension axis (as modelled in *Figure 10* and evaluated in *Figure 11*). This expectation is contrary to experimental observation (compare *Figures 9* and *11*). We consider the alternative mechanisms for the introduction of a preferred molecular alignment in these liquid crystal elastomers in the following section.

MECHANICAL PROPERTIES

The crosslinked liquid crystal polymers considered here do, as was described earlier, behave in the isotropic phase in a similar manner to conventional elastomers[8]. However, in the nematic liquid crystal phase, their mechanical properties are considerably different[12], as has been observed in some siloxane-based liquid crystal elastomers[19].

These mechanical properties are both temperature and time dependent. We shall first consider the time dependency. To illustrate the basic properties we will consider quite rapidly applying a stress via tension to the sample, and then holding the sample at that fixed extension and monitoring the force. In general we would

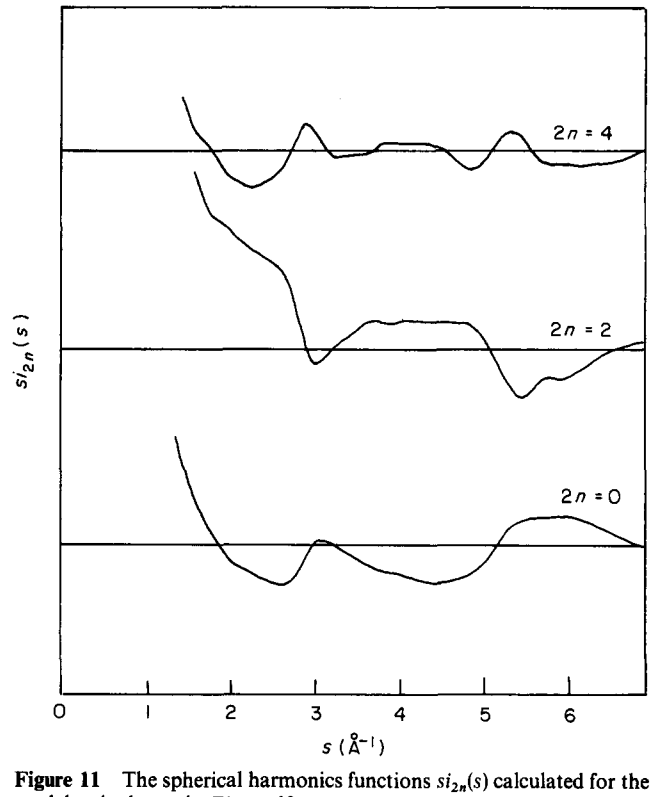

Figure 11 The spherical harmonics functions $si_{2n}(s)$ calculated for the model unit shown in *Figure 10*

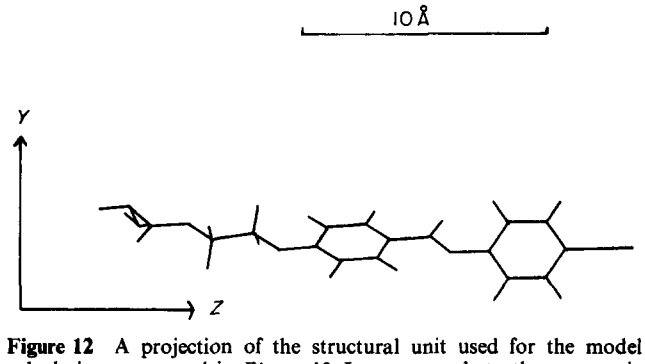

Figure 12 A projection of the structural unit used for the model calculations presented in *Figure 12*. It corresponds to the mesogenic side-chain (as in *Figure 10*) but aligned (the C–N bond) parallel to the extension axis

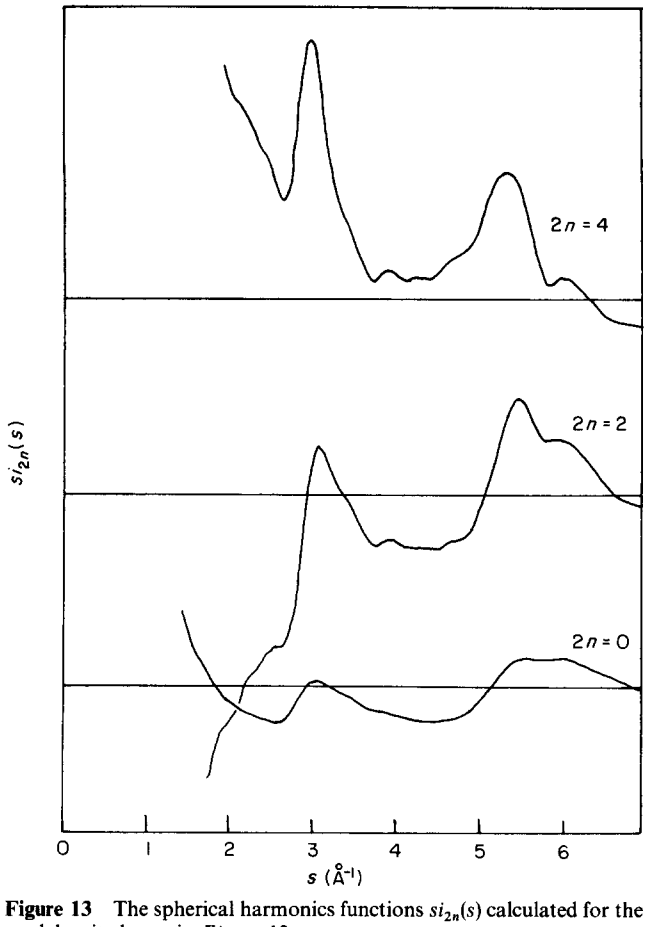

Figure 13 The spherical harmonics functions $si_{2n}(s)$ calculated for the model unit shown in *Figure 12*

expect, in such an experiment, the force to rise with extension, probably accompanied by some development of molecular orientation, and, on holding, for the force to drop a certain amount. That drop would be associated with the relaxation of the structure due to the viscoelastic properties of polymers. It would also be associated with the reduction of the level of molecular orientation. In *Figure 15* we show the measured force as a function of time for the experiment described above. The initial rise is associated with an extension for 10 s at a strain of 0.01 s^{-1}. The drop in force occurs after the cessation of extension. It drops rapidly and reaches a steady value after some 100 s; this would appear in accord with our expectations. However, if we now examine samples prepared in this manner by using wide-angle X-ray scattering techniques to measure the level of preferred orientation, we find a somewhat striking result. At a point just before the extension is halted the measured orientation parameter $\langle P_2 \rangle \approx 0$, while after the force has reduced and reached a steady level the orientation parameter $\langle P_2 \rangle$ has reached *ca.* 0.4. Thus the drop in force is accompanied by an increase in the level of molecular orientation rather than a decrease. Since we have shown that the mesogenic units are aligned parallel to the extension axis, it would appear reasonable that the mesogenic units have become aligned in response to the stress field developed initially rather than due to a coupling to the extension of the molecular network. In other words the application of a stress field to a liquid crystal polymer results in a mechanically induced molecular switching[12] in an analagous manner to that observed following the application of electric or magnetic fields[20,21]. However, the coupling of such a stress field is via the shape anisotropy of the mesogenic units rather than the dielectric or magnetic susceptibility anisotropy. If we remove the stress field completely, but maintain the sample at constant temperature within the nematic phase,

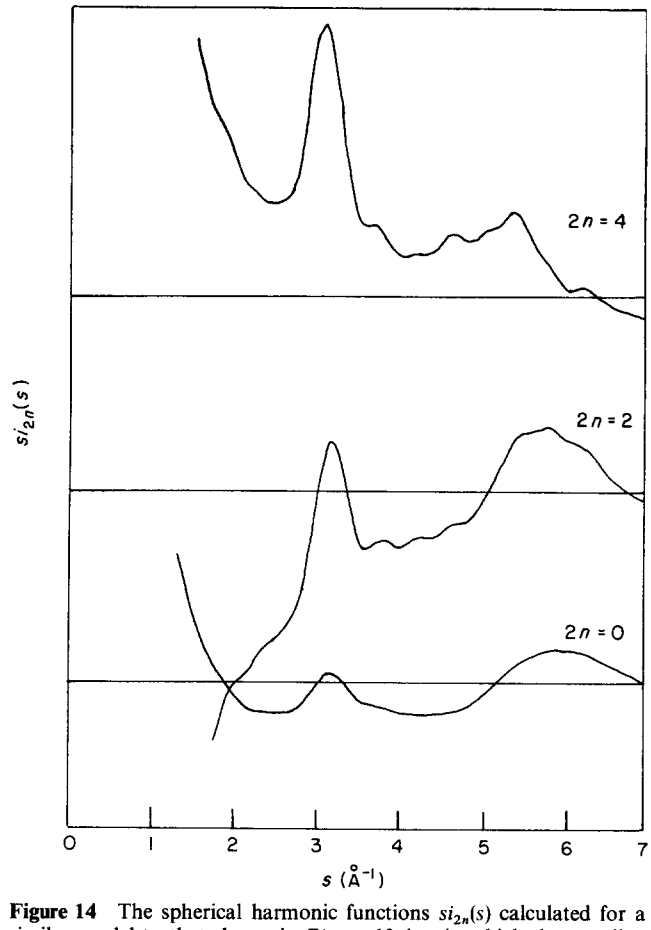

Figure 14 The spherical harmonic functions $si_{2n}(s)$ calculated for a similar model to that shown in *Figure 12*, but in which the coupling chain adopts a *gauche* conformation. The alignment of the mesogenic unit remains the same

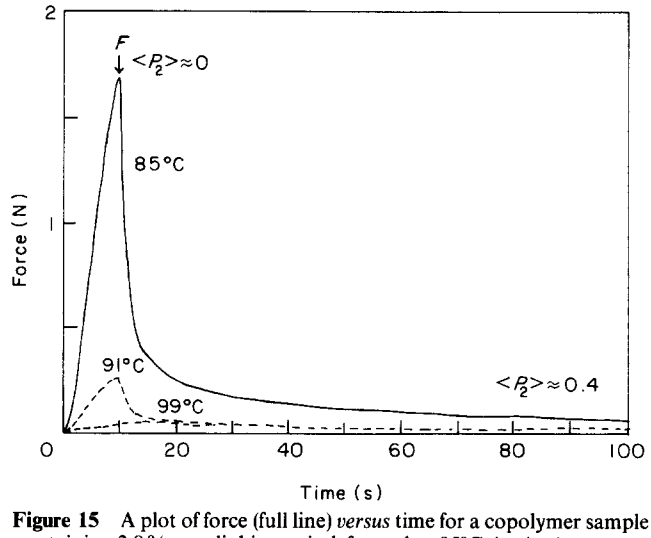

Figure 15 A plot of force (full line) *versus* time for a copolymer sample containing 2.8% crosslinking unit deformed at 85°C, i.e. in the nematic state. The sample was extended continuously for 10 s at a strain rate of 0.01 s^{-1}. The extension was stopped at the point indicated by *F*. The remainder of the curve corresponds to the measured force on the sample held at constant extension ratio of 1:1. The orientation parameter $\langle P_2 \rangle$ was measured by using wide-angle X-ray scattering techniques as described in the text. The broken lines correspond to similar experiments, but made for different sample temperatures

the molecular orientation switches off. The time scale of switching off is at least an order of magnitude longer than the switch on, which parallels the electric and magnetic field effects observed in liquid crystal materials.

If we continue the analogy, then increasing the strength of the stress field should decrease the switching time and enhance the resultant level of molecular orientation. Conversely, decreasing the stress field should slow the response and reduce the level of molecular orientation. Initial experiments give support to these concepts, and a more complete account will be reported when those studies are completed. However, the closeness of the glass transition to the nematic–isotropic transition temperature also results in considerable variation of the stress levels reached for changing sample temperatures. As an illustration we show in *Figure 15* the results of similar experiments to that described above, but made at higher temperatures. As the operating temperature is increased, the stress level reached for an extension of 10% drops considerably. The orientation parameters measured for samples aligned in this manner reflect the drop in the initial applied stress level. If similar experiments are made in the isotropic phase, then the resultant orientation parameter is very small, $\langle P_2 \rangle \approx 0.05$, indicating the critical role of the cooperative liquid crystal molecular organization.

We have monitored more closely the effects of the initial deformation upon the resultant level of molecular orientation, by subjecting the samples to differing extensions at the same temperature (in the nematic phase) and *Figure 16* shows the results. The orientation parameter, $\langle P_2 \rangle$, is plotted for samples that have reached a steady force level after *ca.* 100 s. The ordinate is the extension ratio applied during the initial deformation and held constant upon cessation of strain. In fact, *Figure 15* shows the force to be almost linear with extension, and so the shape of the curve in *Figure 16* would remain the same if plotted as a function of initial stress level reached. The results show that very little deformation (as low as an extension ratio of 3%) will result in molecular switching. The global orientation parameter $\langle P_2 \rangle$ rises with increasing initial stress level until a plateau value is reached. This value corresponds to an alignment of the 'directors' of the nematic structure, and the orientation parameter reflects the distribution of mesogenic units about the common director axis. This final value will be a function of the operating temperature in the same way that the 'order parameter' varies with temperature in conventional liquid crystal systems.

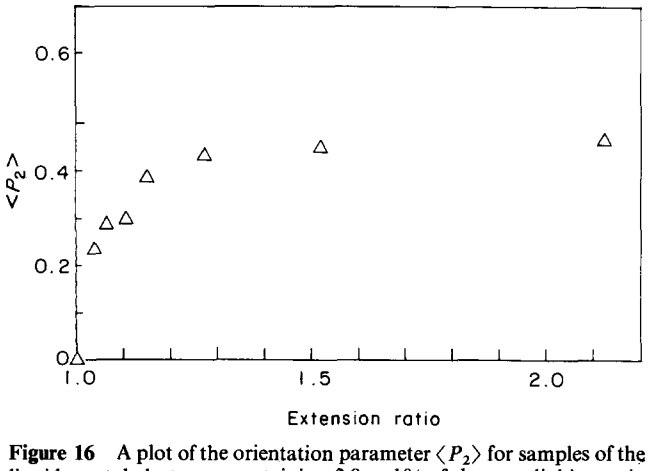

Figure 16 A plot of the orientation parameter $\langle P_2 \rangle$ for samples of the liquid crystal elastomer containing 2.8 mol% of the crosslinking unit, subjected to different initial extensions at 85°C and at a strain rate of $0.01\,s^{-1}$. The samples were allowed to reach a steady force value while held at that indicated extension before rapidly cooling to the glassy state and subsequent orientation measurement. The ordinate corresponds to the extension applied

SUMMARY

The liquid crystal polymer system considered in this study has close coupling between the mesogenic group and the polymer backbone. It is perhaps surprising, therefore, that significant levels of crosslinking can be introduced before enantiotropic liquid crystal phases are not observed. It is clear from the X-ray scattering analysis that the molecular organization is considerably disordered: in particular, the coupling chains adopt non-extended chain conformations. The application of a static stress field induces a molecular reorientation process involving the mesogenic units. These units are aligned parallel to the stress field. The alternative mechanism for alignment via extension of the polymer network and hence a perpendicular alignment of the mesogenic units is not observed. It may be the case that large-scale extension, i.e. $\lambda \gg 2$ would result in such a perpendicular alignment as has been observed in one particular siloxane-based liquid crystal elastomer[19]. The presence of a high population of *gauche* isomers in the coupling chains in macroscopically aligned samples supports the notion that the backbone chain alignment is considerably lower, as indicated in other liquid crystal polymer systems by neutron scattering[3,22]. The stress-induced molecular switching appears to be analagous in many respects to that observed in electric and magnetic fields.

ACKNOWLEDGEMENTS

We thank the University of Reading for the provision of a Fellowship for FJD and the Science and Engineering Research Councils' Electroactive Polymer Programme (GR/D25484) for support. The active involvement of Dr A. Gilbert and Dr J. Mann of the Chemistry Department, Reading, is gratefully acknowledged.

REFERENCES

1 Plate, N. A., Freidzon, Ya. S. and Shibaev, V. P. *Pure Appl. Chem.* 1985, **57**, 1715
2 Finkleman, H. in 'Polymer Liquid Crystals' (Eds A. Ciferri, W. R. Krigbaum and R. B. Meyer), Academic Press, New York, 1982
3 Kirste, R. G. and Ohm, H. G. *Makromol. Chem., Rapid Commun.* 1985, **6**, 179
4 Goozner, R. E. and Finklemann, H. *Makromol. Chem.* 1985, **186**, 2407
5 Barnes, N. R. and Mitchell, G. R. to be submitted to *Liquid Crystals*
6 Finkelman, H., Kock, H. and Rehage, G. *Makromol. Chem., Rapid Commun.* 1981, **2**, 317
7 Davis. F. J., Gilbert, A., Mann, J. and Mitchell, G. R. *Chem. Commun.* 1986, 1333
8 Davis, F. J. and Mitchell, G. R. to be submitted to *Liquid Crystals*
9 Strzelecki, L. and Liebert, L. *Bull. Soc. Chim. Fr.* 1973, 597
10 Treloar, L. R. G. 'The Physics of Rubber Elasticity', Clarendon Press, Oxford, 1975

11 Mitchell, G. R. and Ashman, A. S. in preparation
12 Davis, F. J. and Mitchell, G. R. *Polymer* 1987, **28**, (*Commun.*), 8
13 Mitchell, G. R. and Windle, A. H. *Colloid Polym. Sci.* 1982, **260**, 754
14 Mitchell, G. R. and Windle, A. H. *Polymer* 1983, **24**, 1513
15 Mitchell, G. R. in 'Order in the Amorphous State of Polymers' (Eds S. E. Keinath, R. L. Miller and J. K. Rieke), Plenum, New York, 1986
16 Lovell, R. and Mitchell, G. R. *Acta Cryst.* 1981, **A37**, 135
17 Baumeister, U., Hartung, H. and Jaskolski, M. *Molec. Cryst. Liq. Cryst.* 1982, **88**, 167
18 Vani, G. V. *Mol. Cryst. Liq. Cryst.* 1983, **98**, 275
19 Kock, H. J., Finklemann, H., Gleim, W. and Rehage, G. in 'Polymer Liquid Crystals' (Ed. A. Blumstein), *Polym. Sci. and Technol. Ser* Plenum, New York, **28**, 1983
20 Tal'roze, R. V., Shibaev, V. P. and Khokhlov, A. R. *Makromol. Chem.* 1985, **186**, 1951
21 Simon, R. amd Coles, H. J. *Polymer* 1986, **27**, 811
22 Keller, P., Carvlho, B., Cotton, J. P., Lambert, M., Moussa, F. and Pepy, G. *J. Phys. Lett., Paris* 1985, **46**, L-1065